# Phase locking and quantum statistics in a parametrically driven nonlinear resonator

G. H. Hovsepyan,[1,2,*] A. R. Shahinyan,[1,2,†] Lock Yue Chew,[3,4,‡] and G. Yu. Kryuchkyan[2,5,§]

[1]*Institute for Physical Research, National Academy of Sciences, Ashtarak-2, 0203 Ashtarak, Armenia*

[2]*Centre of Quantum Technologies and New Materials, Yerevan State University, 1 Alex Manoogian Street, 0025 Yerevan, Armenia*

[3]*School of Physical and Mathematical Sciences, Nanyang Technological University, 21 Nanyang Link, Singapore 637371*

[4]*Complexity Institute, Nanyang Technological University, 18 Nanyang Drive, Singapore 637723*

[5]*Armenian State Pedagogical University after Kh. Abovyan, 17 Tigran Mets Street, 0010 Yerevan, Armenia*

(Received 3 November 2015; revised manuscript received 29 February 2016; published 29 April 2016)

We discuss phase-locking phenomenon at low-level of quanta and quantum statistics for parametrically driven nonlinear Kerr resonator (PDNR). Oscillatory mode of PDNR is created in the process of a degenerate down-conversion of photons under interaction with a train of external Gaussian pulses. We calculate the distribution of photon-number states, the second-order correlation function of photons, the Wigner functions of cavity mode showing two-fold symmetry in phase space, and we analyze formation of phase-locked states in the regular as well as the quantum chaotic regime of the PDNR.

DOI: 10.1103/PhysRevA.93.043856

## I. INTRODUCTION

The parametric phase-locked oscillators are known to possess a wide-ranging set of applications in both the fundamental and the applied sciences. In recent years, this device has become a significant part in the experimental implementation of basic quantum optical systems and it is also envisaged to be a core component of quantum computers [1,2]. The simplest realization of such systems displaying phase-locking behavior is the one-mode optical parametric oscillator (OPO), which has been shown to be an efficient source of squeezed light [3]. The subharmonic oscillatory mode of the OPO excited through the degenerate down-conversion process is found to exhibit two-phase stability. This indicates the presence of two stable states in the optical mode above the generation threshold, with the two states having equal photon number but different phases [4–6]. As a result, the Wigner function of the subharmonic mode acquires a twofold symmetry in phase space.

Such phase-locking behavior can also be realized in the nondegenerate (double-resonance) optical parametric oscillator by including an additional intracavity quarter waveplate to provide polarization mixing between two orthogonally polarized modes of the subharmonics [7–9]. A full quantum mechanical treatment of this system has been presented in [10,11] on the generation of continuous-variable entangled states of light beams under mode phase-locked condition, while experimental realizations have been achieved in [12–14]. The experimental observation of dynamical signatures of the self-phase-locking phenomenon in a triply resonant degenerate OPO was reported in [15]. On the other hand, the cascaded phase-locked oscillators for the production of three-photon states were proposed in [16–19].

The phase-locking transition was also observed in a chirped superconducting Josephson resonator [20]. More recently, the Josephson parametric phase-locked oscillator was demonstrated and it was applied to detect binary signals with the identified digital information stored in the form of two oscillatory distinct phases [1]. This enables the accurate measurement of the state of a superconducting qubit without affecting the integrity of the stored information.

Another important implementation that exploits the phase-locking mechanism is the combination of the OPO with the intracavity Kerr nonlinear element, the so-called parametrically driven nonlinear resonator (PDNR) [21,22]. This system was first proposed as an optical parametric oscillator in the pulsed regime with the incorporation of an intracavity third-order nonlinear element leading to Kerr interaction [23]. A complete quantum treatment of the phase-locked PDNR has been developed in terms of the Fokker-Planck equation in the complex $P$ representation [24–26]. The quantum regime of PDNR requires a comparatively high level of third-order Kerr nonlinearity with respect to dissipation. In this regime, the pulsed PDNR has been proposed for the production of quantum superposition states and two-photon Fock states [27].

Up till now, the phenomenon of phase locking has been examined mainly from the mean-field approach, which is fully justifiable in the case of a relatively high photon number of cavity modes as well as for the regular operational regimes of parametric devices, for instance, via the use of continuous-wave or pulsed driving fields. In this paper we investigate phase locking at a low level of excitation number of the cavity mode, in the strong quantum regime, and in complete consideration of dissipation and quantum fluctuations. Moreover, we analyze phase locking within the chaotic regime of the PDNR. In other words, we study properties of dissipative chaos for oscillatory open systems that display phase-locking behavior.

The most successful approach of probing quantum dissipative chaos is based on quantum tomographic methods, which involve measurements of the Wigner function in phase space. In consequence, quantum chaos can be detected through a comparison between the contour plots of the Wigner functions and the strange attractors that characterize dissipative chaos in the classical Poincaré section [28–31]. Note that such an analysis seems to be qualitative rather than quantitative for the range of low-level oscillatory excitation numbers, where the validity of the semiclassical equation is questionable.

*gor.hovsepyan@ysu.am

†anna_shahinyan@ysu.am

‡lockyue@ntu.edu.sg

§kryuchkyan@ysu.am

 

Nevertheless, we discuss the semiclassical approach to chaos by using the Poincaré section with a quantum analysis of phase locking for both the regular and chaotic regimes based on the Wigner functions. Moreover, the various regimes of the PDNR will be clarified through consideration of quantum statistical effects on the basis of the second-order photon correlation function at coinciding times, the probability distribution of the photon-number states, and the quantum purity of states. Note that alternative approaches of probing quantum dissipative chaos involve consideration of entropic characteristics: analysis of the statistics of the excitation number [32,33], application of methods based on fidelity decay [34–36], the Kullback-Leibler quantum divergence [37], and the purity of quantum states [38].

Our paper is arranged as follow. In Sec. II we provide a brief description of the PDNR driven by a train of Gaussian pulses. In Sec. III we study the phase-locking phenomenon at a low-level of excitation number and the quantum statistics of the mode for both the regular and chaotic regimes of the PDNR. Finally, we summarize our results in Sec. IV.

## II. THE PDNR IN THE PULSED REGIME: TWOFOLD SYMMETRY

We consider a composite nonlinear one-mode resonator involving second-order and third-order Kerr nonlinearities excited by a train of pulses. The system is thus a parametrically driven Kerr resonator with the following Hamiltonian:

$$H = \hbar\omega_0 a^\dagger a + \hbar\chi(a^\dagger a)^2 + \hbar f(t)(\Omega e^{-i\omega t} a^{\dagger 2} + \Omega^* e^{i\omega t} a^2) + H_{\rm loss}. \quad (1)$$

Here $a^\dagger$ and $a$ are the oscillatory creation and annihilation operators, respectively, $\omega_0$ is the oscillatory frequency, $\omega$ is the mean frequency of the driving field, and $\chi$ is the strength of the nonlinearity, which is proportional to the third-order susceptibility for the case of Kerr media. The coupling constant $\Omega f(t)$ is proportional to the second-order susceptibility and the time-dependent amplitude of the driving field. It consists of Gaussian pulses with duration $T$ separated by time interval $\tau$ as follows:

$$f(t) = \sum_{n=0}^{\infty} e^{-(t-t_0-n\tau)^2/T^2}. \quad (2)$$

Note that $H_{\rm loss} = a\Gamma^\dagger + a^\dagger\Gamma$ is responsible for the linear loss of the oscillatory mode due to coupling to a heat reservoir, which gives rise to a damping rate of $\gamma$.

We describe the dissipative dynamics of the PDNR with the master equation. The reduced density operator of the oscillatory mode $\rho$ obeys the transformation $\rho \to e^{-i(\omega/2)a^\dagger a t}\rho e^{i(\omega/2)a^\dagger a t}$ in the interaction picture. It is governed by the following master equation:

$$\frac{d\rho}{dt} = -\frac{i}{\hbar}[H_0 + H_{\rm int}, \rho] + \sum_{i=1,2}(L_i\rho L_i^\dagger - \tfrac{1}{2}L_i^\dagger L_i\rho - \tfrac{1}{2}\rho L_i^\dagger L_i) \quad (3)$$

within the framework of the rotating-wave approximation. Note that $L_1 = \sqrt{(N+1)\gamma}a$ and $L_2 = \sqrt{N\gamma}a^\dagger$ are the Lindblad operators, $\gamma$ is the dissipation rate, and $N$ denotes the mean number of quanta of the heat bath. Furthermore,

$$H_0 = \hbar\Delta a^\dagger a, \qquad H_{\rm int} = \hbar\chi(a^\dagger a)^2 + \hbar f(t)(\Omega a^{\dagger 2} + \Omega^* a^2), \quad (4)$$

with $\Delta = \omega_0 - \omega/2$ the detuning between the half frequency of the driving field $\omega/2$ and the oscillatory frequency $\omega_0$. To study pure quantum effects, we focus on cases of very low reservoir temperature for which the mean number of reservoir photons $N = 0$.

Various realizations of the Kerr resonator excited by the parametric two-photon process have been proposed. Recent progress in circuit QED, superconducting systems, and solid-state artificial atoms has opened up new avenues for the design of device configurations based on our model. In this direction, one of the most promising systems consists of a quarter-wave coplanar microwave cavity and a superconducting quantum interference device (SQUID) [39,40]. By replacing the single junction with a SQUID, the Kerr coefficient then allows the parametric term to describe a degenerate two-photon excitation by microwave light [40]. The experimental realization has been reported in [1]. It was demonstrated that this system can be described as a PDNR with a Hamiltonian given by Eq. (1) where $f(t) = 1$ [1,26,40,41]. In this case, the raising $a^\dagger$ and lowering $a$ operators in Eq. (1) describe the normal modes of the resonator plus junction circuit, while the quadratic part of the Josephson potential leads to self-Kerr nonlinear effects.

We solve the master equation given by Eq. (3) numerically based on the method of quantum state diffusion (QSD) [42]. According to this method, the reduced density operator is calculated as the ensemble mean

$$\rho(t) = M[|\psi_\xi(t)\rangle\langle\psi_\xi(t)|] = \lim_{N\to\infty}\frac{1}{N}\sum_{\xi}^{N}|\psi_\xi(t)\rangle\langle\psi_\xi(t)| \quad (5)$$

over the stochastic states $|\psi_\xi(t)\rangle$ describing evolution along a quantum trajectory. The stochastic equation for the state $|\psi_\xi(t)\rangle$ involves the Hamiltonian given by Eq. (1) and the Lindblad operators of the noise terms from the master equation (3).

We calculate the density operator using an expansion of the state vector $|\psi_\xi\rangle$ in a basis of Fock's number states of the resonator mode. The application of this technique to the studies of driven nonlinear oscillators and OPOs can be gleaned from Refs. [28–30,32,33].

After we obtain $\rho$, the mean photon number, the distribution of oscillatory excitation states $P(n) = \langle n|\rho|n\rangle$, the purity of states, the normalized second-order correlation function $g^{(2)}$, and the Wigner functions will be calculated in the framework of the QSD method.

In the semiclassical approach, the corresponding equation of motion for the dimensionless amplitude of oscillatory mode takes the following form:

$$\frac{d\alpha}{dt} = -i[\Delta + \chi + 2|\alpha|^2\chi]\alpha - 2if(t)\Omega\alpha^* - \frac{1}{2}\gamma\alpha. \quad (6)$$

This equation modifies the standard equation for parametric oscillator with Kerr nonlinearity for the case of pulsed excitation. The semiclassical steady-state solutions and stability properties of the PDNR for the monochromatic excitation

$f(t) = 1$ have been presented in [24,25]. In standard analysis, the amplitude of the oscillatory mode is described by $\alpha = n^{1/2}\exp(i\varphi)$ in terms of the intensity $n$ (in photon-number units) and the phase of the mode $\varphi$, with the semiclassical steady-state solutions obtained in the over-transient regime and for large oscillatory mean excitation number $n \gg 1$. Note that the amplitude of the driving field is represented as $\Omega = I^{1/2}\exp(i\Phi)$, where $I$ is the intensity and $\Phi$ is the corresponding phase. In this case, the above-threshold regime takes place when $I > I_{\rm th} = \frac{\gamma^2}{\Omega^2}(1 + \frac{\Delta^2}{\gamma^2})$. The system displays regular behavior of photon number $n$ versus $I$ for positive detunings. On the other hand, the bistable regime is realized for negative detunings. In the regular above-threshold regime, there actually exist two stable steady states with equal intensities but opposite phase:

$$\varphi = \tfrac{1}{2}\Phi \pm \pi m, \tag{7}$$

indicating the formation of phase locking with twofold symmetry.

It is well known that the phase-locking phenomenon reflects the twofold symmetry of the Wigner function, which has been demonstrated in the steady-state regime of the OPO under monochromatic driving [16,17,19]. The situation of phase locking with twofold symmetry also arises for the composite system under consideration due to the quadratic form of the nonlinear term in the Hamiltonian for the pulsed PDNR given by Eq. (1). Indeed, by considering the transformations

$$H' = U^{-1}HU, \quad \rho' = U^{-1}\rho U \tag{8}$$

with the unitary operator

$$U = \exp(i\theta a^\dagger a), \tag{9}$$

we have verified that the Hamiltonian of Eq. (1) and the density operator of the oscillatory mode satisfy the following commutation relations:

$$[H,U] = 0, \tag{10}$$

$$[\rho(t),U] = 0, \tag{11}$$

if the parameter $\theta = \pi$. It is easy to demonstrate that the Wigner function of the oscillatory mode expressed through the density operator

$$W(\alpha) = \frac{1}{\pi^2}\int d^2\gamma\, \mathrm{Tr}(\rho e^{\gamma a^\dagger - \gamma^* a})e^{\gamma^*\alpha - \gamma\alpha^*} \tag{12}$$

displays twofold symmetry in its rotation around the origin of the phase space:

$$W(r,\theta+\pi) = W(r,\theta). \tag{13}$$

Note that the polar coordinates $(r,\theta)$ are related to the complex plane $X = (\alpha + \alpha^*)/2 = r\cos\theta$ and $Y = (\alpha - \alpha^*)/2i = r\sin\theta$. This result is obtained in the general form for arbitrary time-dependent amplitudes of the external field and for all operational regimes of the PDNR. In fact, such twofold symmetry persists in the Wigner functions when the PDNR is taken in the quantum chaotic regime, which will be discussed in the next section.

In the following we consider the phase-locking phenomenon based on the Wigner functions in phase space within both the regular and chaotic regimes of the PDNR. The Wigner function is determined by averaging an ensemble of quantum trajectories for a definite time instant according to the following formulation:

$$W(r,\theta) = \sum_{n,m}\rho_{nm}(t)W_{mn}(r,\theta), \tag{14}$$

with the calculation of the matrix elements $\rho_{nm} = \langle n|\rho|m\rangle$ of the density operator in the Fock state representation. Here the coefficients $W_{mn}(r,\theta)$ are the Fourier transform of the matrix elements of the Wigner characteristic function.

By analyzing the operational regimes of the PDNR driven by the pulse train, we have concluded that the regular regime is mainly realized for positive detunings $\Delta > 0$, while the chaotic dynamics takes place for negative detunings $\Delta < 0$. This result is in accord with the above discussion on the case of monochromatic excitation of the PDNR that exhibits bistability only for negative detuning. It is known that one of the scenarios of the transition to chaos is realized through a bistable regime of the nonlinear system. In this way, the nonlinear system driven by the train of pulses in the range of bistability oscillates between the two possible metastable states. Then, for definite parameters leading to strong mixing of these states, the system becomes chaotic. Indeed, just for the case of negative detuning, the presence of the pulse train has served to control the transition from bistable behavior to chaotic dynamics with respect to the semiclassical solution. In fact, for chaos to happen, the other parameters of our model have to satisfy the following criteria: $\Omega \simeq |\Delta|$ and $\pi/2 \leqslant \tau/T \leqslant 2\pi$. It should be noted that the above conditions are specific to the pulsed PDNR, since for the standard pulse-driven anharmonic oscillator without a parametric term, quantum chaotic regimes are realized for both signs of the detuning. The typical results for the Wigner functions corresponding to the cases of positive and negative detunings for the pulse-driven PDNR are illustrated in Figs. 2–4.

## III. PHASE LOCKING AND QUANTUM STATISTICS IN THE ORDER-TO-CHAOS TRANSITION

In this section we analyze the phase-locking phenomenon by determining the time-dependent excitation numbers, second-order correlation function, and Wigner function of the oscillatory mode. We calculate these quantities by averaging over an ensemble of quantum trajectories for definite time instants and with respect to the parameters $\Delta/\gamma$, $\chi/\gamma$, and $\Omega/\gamma$ as well as the parameters of the pulses corresponding to the regular and chaotic regimes. Note that all ensemble-averaged quantities are nonstationary and exhibit a periodic time-dependent behavior, i.e., they follow the periodicity of the driving pulses beyond the transient state of the system.

### A. Monitoring of phase locking on the Wigner functions

Calculations have shown that the PDNR in the pulsed regime under quantum treatment displays regular behavior only for positive detunings $\Delta > 0$, while a chaotic dynamics is realized for negative $\Delta < 0$ detunings. Specifically, the typical results on the dynamics of the photon number are presented in Fig. 1 for negative and positive values of the detuning

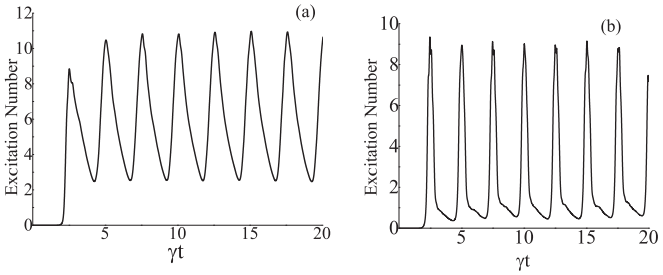


FIG. 1. Excitation number against time intervals for the negative and positive detuning. The parameters used are $\chi/\gamma = 1$, $\Omega/\gamma = 20$, $T = 0.5\gamma^{-1}$, $\tau = 4\pi\gamma^{-1}/5$, and (a) $\Delta/\gamma = -20$ and (b) $\Delta/\gamma = 20$.

corresponding to the chaotic [Fig. 1(a)] and regular regimes [Fig. 1(b)]. We observe that the system operates in the strong quantum regime at a level of small excitation number for these parameter values. The ensemble-averaged mean excitation number is clearly regular in both regimes. It demonstrates the well-known result that the quantum dissipative chaotic dynamics is not evident in the dynamics of the mean oscillatory number. Nonetheless, it is possible to detect quantum chaotic behavior from other physical quantities, in particular, the Wigner function.

In Fig. 2 we present our results on the Wigner function in the strong quantum regime for both the regular and chaotic behavior of the PDNR. Note that the results were selected

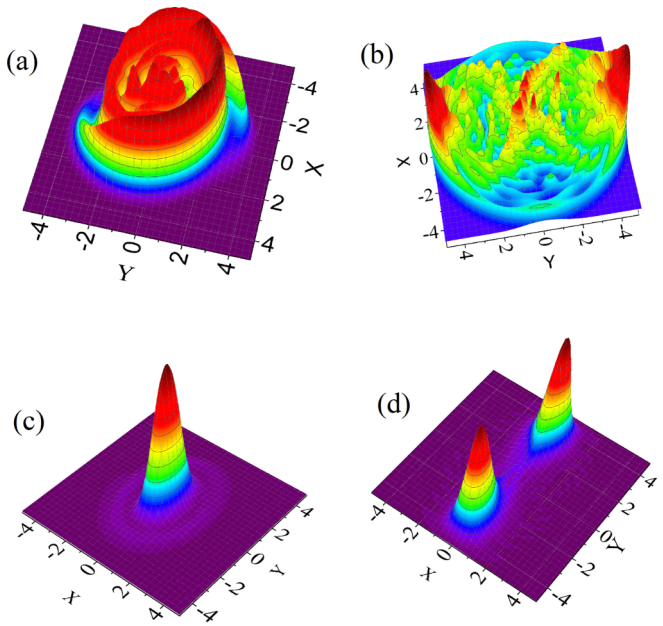


FIG. 2. Wigner functions for the positive and negative detunings at time instants corresponding to (a) and (c) the minimum and (b) and (d) the maximum of the excitation number observed in Fig. 1. The parameters employed are (a) and (b) $\Delta/\gamma = -20$, $\chi/\gamma = 1$, $\Omega/\gamma = 20$, $T = 0.5\gamma^{-1}$, and $\tau = 4\pi\gamma^{-1}/5$ and (c) and (d) $\Delta/\gamma = 20$, $\chi/\gamma = 1$, $\Omega/\gamma = 20$, $T = 0.5\gamma^{-1}$, and $\tau = 4\pi/5\gamma^{-1}$. Note that (a) and (c) relate to the minimal value of the photon number, while (b) and (d) relate to the maximal value. The Wigner functions of (a) and (b) are for the chaotic regime, while (c) and (d) are for the regular regime of the PDNR.

at definite moments in time that correspond to the minimal and maximal values of the mean excitation number depicted in Fig. 1. We observe that all the Wigner functions display twofold symmetry in phase space according to Eq. (13). In particular, Figs. 2(c) and 2(d) show the formation of phase-locked states for the regular regime as the photon number of the oscillatory mode increases. The single-peaked Wigner function that occurs at the minimum of the excitation number $n_{\min} = 1$ is squeezed in phase space [see Fig. 2(c)], indicating the formation of squeezed states in the oscillatory mode. By increasing the excitation number, we observe the formation of two squeezed humps [see Fig. 2(d)] at the maximum of the excitation number $n_{\max} = 9$. The two humps correspond to two states of equal photon number, but with two different phases of the cavity mode of the PDNR, which is above the generation threshold of the semiclassical approach. We note that the distance between the two humps depends on the excitation number of the optical mode. Interestingly, our results have uncovered the occurrence of phase-locking behavior at relatively small excitation numbers.

In general, the definition of the threshold $I_{\text{th}}$ as a critical point commonly emerges from the analysis of semiclassical solutions and their stability regions. Based on quantum theory, as the relative nonlinearity $\chi/\gamma$ increases, the semiclassical characteristic threshold behavior, which is determined by a drastic increase of the intensity in the transition region, disappears. Thus, for the parameters used in Fig. 2, there occurs a critical or threshold range, instead of a threshold point [24–26].

Our results for the case of negative detuning are depicted in Figs. 2(a) and 2(b) for time instants that correspond to the minimal and maximal values of the excitation number [see Fig. 1(a)]. The latter result is cardinally different from the Wigner function obtained for the regular operational regime. While the contour plots of the Wigner function for regular dynamics are clearly bell shaped and localized in a narrow region of phase space, the phase-space distribution for the case of negative detuning is observed to be wider. In fact, we also observe a broadening of the corresponding excitation number distribution $P(n)$ (see Sec. III C). The shape of the distribution is found to change irregularly depending on the duration $T$ and time interval $\tau$ between pulses. We conjecture that these Wigner functions depict the chaotic behavior of PDNR in the strong quantum regime.

A detailed identification of quantum chaos based on a comparison between the contour plots of the Wigner function and the corresponding classical Poincaré section has been performed for the standard nonlinear resonator driven by a train of periodic pulses [30]. It was demonstrated in [30] that for comparatively small values of the ratio $\chi/\gamma$, the contour plots of Wigner functions are relatively similar to the strange attractors in the Poincaré section. Analogous consideration for the PDNR will be presented below in Sec. III B.

By analyzing the behavior of phase locking in the chaotic regime of the PDNR, we can easily conclude that the Wigner function exhibits twofold symmetry under a rotation of angle $\pi$ around its origin in phase space based on the general formula given by Eq. (13). Thus, the parametric interaction of the cavity mode in the PDNR is observed to display twofold symmetry in the phase space for both operational regimes. The Wigner

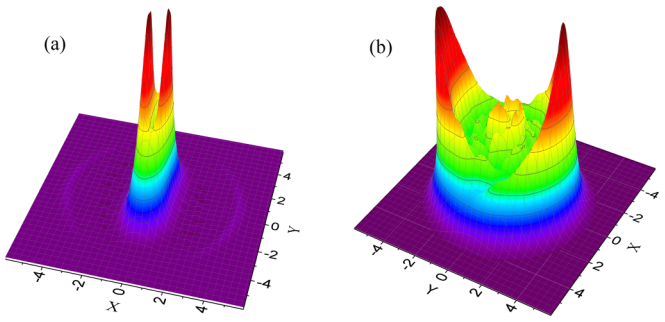


FIG. 3. Wigner function for the case of positive and negative detuning and for a time instant of mean excitation number that lies between the minimal and maximal values. The parameters used are $\chi/\gamma = 1, \Omega/\gamma = 20, T = 0.5\gamma^{-1}, \tau = 4\pi\gamma^{-1}/5$, and (a) $\Delta/\gamma = 20$ and (b) $\Delta/\gamma = -20$.

function in Fig. 2(a) has the form of a broken one-peaked localized state, while the two maxima at the Wigner function of Fig. 2(b) reflect the track of phase-locked states in the quantum chaotic regime.

It is also important to examine the phase-locking behavior by considering the system time evolution. To achieve this goal, we have calculated the Wigner function for time instants that lie between the minimal and maximal values of the excitation number. The results depicted in Fig. 3 show the initial stage of phase splitting of the optical mode for the two phases in both the regular and chaotic regimes.

We found that the above results are typical for the PDNR in strong quantum regime. In Fig. 4 we have presented additional

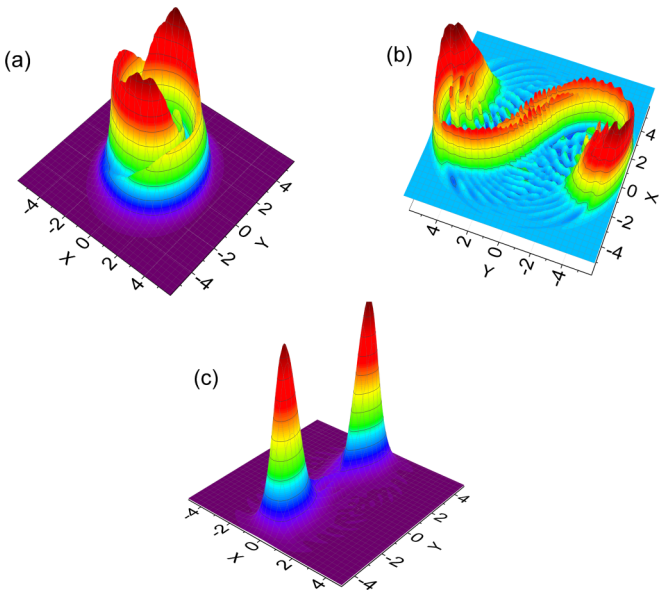


FIG. 4. Wigner functions for negative detuning for time instants that correspond to (a) the minimal and (b) the maximal values of the mean excitation number. The parameters used are $\Delta/\gamma = -7.5, \chi/\gamma = 0.5, \Omega/\gamma = 10, T = 0.25\gamma^{-1}$, and $\tau = 2\pi/5\gamma^{-1}$. Also shown is (c) the Wigner function for the regular regime, with a time instant at the maximal value of the mean excitation number. The parameters employed are $\Delta/\gamma = 15$, $\chi/\gamma = 1$, $\Omega/\gamma = 10$, $T = 0.5\gamma^{-1}$, and $\tau = 2\pi\gamma^{-1}$.

Wigner functions at other parameter values of $\Delta/\gamma$, $\chi/\gamma$, and $\Omega/\gamma$. In particular, we observe that a decrease in the amplitude of the driving field would lead to a decrease in the distance between the humps of the two localized states. This is apparent by comparing the results of Fig. 2(d) with Fig. 4(c) for the regular regime. In the case of quantum chaotic regimes [see Figs. 4(a) and 4(b)], we notice that a slight change in the system parameters can lead to subtle variations in the Wigner function. Indeed, this can be easily observed in Figs. 4(a) and 4(b), where a smaller nonlinearity and field amplitude have been used relative to those employed in Fig. 2.

### B. Semiclassical treatment and the Poincaré section

In the semiclassical limit, chaos is observed in the Poincaré section, which is constructed from the semiclassical trajectory in phase space from the dimensionless position and momentum variables, i.e., $X = \mathrm{Re}(\alpha)$ and $Y = \mathrm{Im}(\alpha)$, respectively, as solutions of Eq. (6). In order to yield the Poincaré section, we have employed the real and imaginary parts of the complex amplitude as an arbitrary initial phase-space point $(X_0, Y_0)$ of the system at time $t_0$. We then define a constant phase map in the $(X, Y)$ plane by the sequence of periodically shifted points $(X_n, Y_n) = [X(t_n), Y(t_n)]$ at $t_n = t_0 + n\tau$ $(n = 0, 1, 2, \ldots)$. In this way, the Poincaré section is expressed through the constant phase map of $(X_n, Y_n)$ in the phase space. If the PDNR is driven by a sequence of short pulses, the dynamics of the system is nonstationary and hence the Poincaré section would depend on the initial time instant $t_0$. We have chosen various initial times $t_0$ in order to ensure proper matching to the corresponding time instants of the Wigner function. It is evident from Eq. (6) that the system possesses symmetry properties in the phase space according to the replacement $\alpha \to (-\alpha)$. We demonstrate below that this phase symmetry is also displayed in strange attractors of the Poincaré section.

The typical results of our calculations in the semiclassical approach are depicted in Fig. 5 for the mean excitation number $|\alpha|^2$ and the Poincaré section for the parameters $\Delta/\gamma$, $\chi/\gamma$, and $\Omega/\gamma$ as well as for the parameters of pulses corresponding to the chaotic regimes. It can be observed that while $|\alpha|^2$ shows the usual chaotic dynamics [see Fig. 5(a)], the Poincaré section [see Fig. 5(b)] displays the structure of the strange attractor.

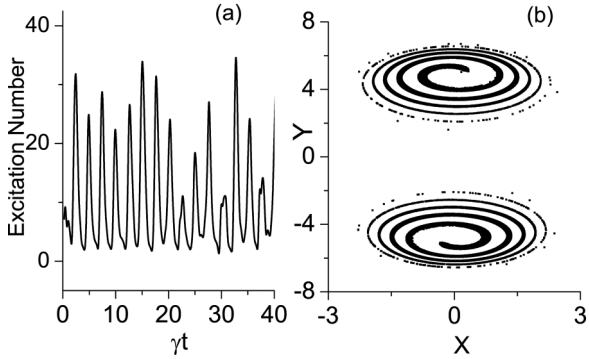


FIG. 5. Semiclassical results for the PDNR: (a) the mean excitation numbers (photon numbers) versus dimensionless scaled time and (b) the Poincaré section. The parameters are $\Delta/\gamma = -10$, $\chi/\gamma = 1$, $\Omega/\gamma = 20$, $T = 0.5\gamma^{-1}$, and $\tau = 4\pi/5\gamma^{-1}$.

Moreover, the Poincaré section is found to be symmetric with respect to rotation by the angle $\pi$ around the origin in the phase space in lieu of the invariance of the operations $X \to -X$ and $Y \to -Y$.

A comparison between the Poincaré section and the Wigner function in the chaotic regime shows that the main difference between them is the existence of fine fractal structures within the Poincaré section, which are absent in the Wigner function. This is due to the Heisenberg uncertainty principle, which prevents sub-Planck structures to appear in phase space. The consequence is a loss of correspondence between the quantum and classical distributions in the deep quantum regime.

### C. Photon-number statistics and quantum purity

In this section we discuss quantum effects in the PDNR for both regular and chaotic regimes on the basis of the second-order photon correlation function at coinciding times

$$g^{(2)} = \frac{\langle a^\dagger a^\dagger a a \rangle}{\langle a^\dagger a \rangle^2}, \tag{15}$$

the photon-number distribution, and the quantum purity. In particular, this analysis can be useful for probing quantum chaos by observing photon statistics.

To achieve our objective, we calculate the correlation function for both the regular and chaotic regimes of the PDNR by employing the two sets of parameters used in Fig. 2, which would lead to approximately equal excitation numbers for each of the regimes. The correlation function is found to be nonstationary and strongly dependent on the properties of the input pulsed driving field. The typical time-dependent behavior of $g^{(2)}$ is illustrated in Fig. 6 corresponding to the chaotic regime [see Fig. 6(a)], which is realized through negative detuning, and to the regular regime for positive detuning [see Fig. 6(b)]. These results show drastically different behavior of the correlation function $g^{(2)}$ for the chaotic and regular regimes of the PDNR.

Let us now discuss the above observations in greater detail. In the regular regime, the minimum value of $g^{(2)}$ equals 1.2 approximately and occurs for time instants corresponding to

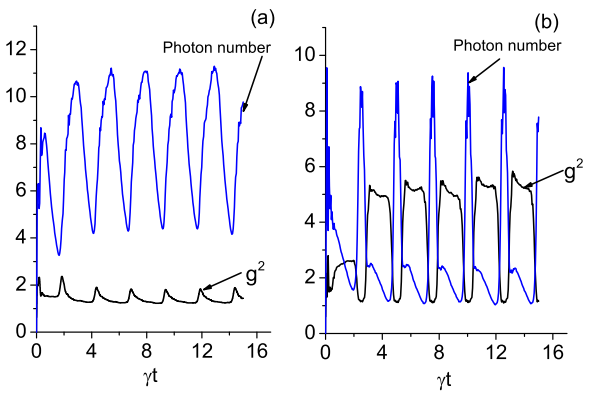


FIG. 6. Averaged photon numbers and the second-order correlation function for both chaotic and regular regimes of the PDNR. The parameters are (a) $\Delta/\gamma = -20$, $\chi/\gamma = 1$, $\Omega/\gamma = 20$, $T = 0.5\gamma^{-1}$, and $\tau = 4\pi\gamma^{-1}/5$ and (b) $\Delta/\gamma = 20$, $\chi/\gamma = 1$, $\Omega/\gamma = 20$, $T = 0.5\gamma^{-1}$, and $\tau = 4\pi/5\gamma^{-1}$.

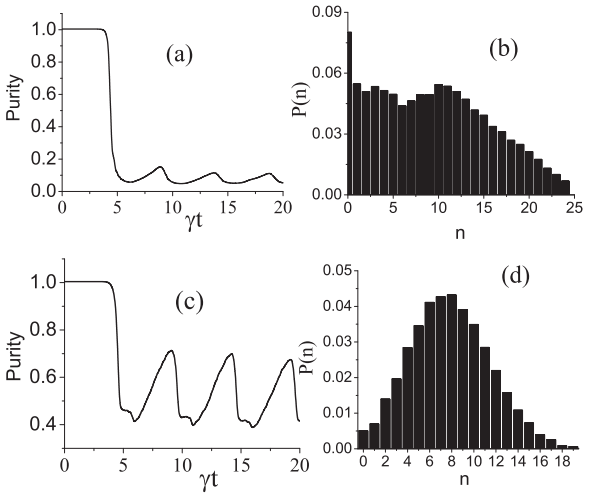


FIG. 7. Time dependence of the quantum purity and distribution of oscillatory excitation numbers for (a) and (b) negative and (c) and (d) positive detunings. The parameters are as follows: (a), (b) $\Delta/\gamma = -20$, $\chi/\gamma = 1$, $\Omega/\gamma = 20$, $T = 0.5\gamma^{-1}$, and $\tau = 4/5\pi\gamma^{-1}$, (c), (d) $\Delta/\gamma = 20$, $\chi/\gamma = 1$, $\Omega/\gamma = 20$, $T = 0.5\gamma^{-1}$, $\tau = 4/5\pi\gamma^{-1}$.

maximum values of the averaged photon numbers. At the maximum of the correlation function, we have $g^{(2)} = 5.2$ for the mean photon number $n = 2.5$. Thus, both results describe the phenomenon of photon bunching as stipulated by the parametric two-photon processes leading to the excitation of cavity mode. These results on photon statistics are in accord with the results of Wigner functions presented in Figs. 2(c) and 2(d) for the same parameters. The Wigner functions of the PDNR for the regular regime displays one-peak structure as well as two localized states at the maximum values of the photon number. The peaks are squeezed in the phase space for the case of photon bunching. In the chaotic regime, the correlation function at the minimum value of the photon number equals 2 approximately, which implies a photon statistic of thermal or chaotic light. For time instants that correspond to the maximum values of the photon number, $g^{(2)}$ is observed to decrease slightly. Note that the corresponding Wigner functions depicted in Figs. 2(a) and 2(b) confirm the chaotic regime of the PDNR. Thus, we conclude that the two-photon processes that stimulate the excitation of mode in the PDNR lead to strong photon-number correlation in the regular regime, but not in the chaotic regime. Nevertheless, this peculiar feature of the PDNR is displayed within the twofold symmetry in the phase space of both operational regimes.

Next we illustrate the distribution function of the oscillatory excitation number $P(n) = \langle n|\rho|n\rangle$ in Figs. 7(b) and 7(d) and the results on quantum purity in Figs. 7(a) and 7(c). It was demonstrated in Ref. [32] that $P(n)$ tends to broaden when a driven anharmonic oscillator transits from the regular to the chaotic regime. We show here that analogous behavior happens for the PDNR. Indeed, we observe that the $P(n)$ for the regular dynamics is bell shaped and localized in a narrow interval of oscillatory number, but the distribution for the chaotic dynamics is flat topped with oscillatory number ranging from $n = 0$ to $n_{\max} = 30$ [see Fig. 7(b)]. In fact, the shape of the latter distribution changes irregularly and depends on the duration $T$ and time intervals $\tau$ between the pulses.

In Figs. 7(a) and 7(c) we plot the corresponding quantum purity versus the scaled time $\gamma t$. Quantum purity is a usual measure of the statistical characteristic of quantum states and decoherence. It is defined through the density matrix $\rho$ of the system as $P = \mathrm{Tr}(\rho^2)$. For any pure state $\mathrm{Tr}(\rho^2) = 1$ and for mixed states it is less than 1.

In general, the purity of an ensemble of oscillatory states strongly depends on the operational regimes of the PDNR. More specifically, an increase in the excitation number would raise the number of mixing oscillatory states, leading to a decrease in purity. In addition, diffusion and decoherence of oscillatory modes are also relevant to the level of purity. Therefore, in our comparative analysis of Figs. 7(a) and 7(c), we consider regimes of regular and chaotic dynamics with the same level of the mean photon number. From the figures we observe a time-dependent modulation of the purity by the pulse train at the over-transient time interval. Comparing the results of the two figures, we conclude that the magnitude of the purity for the chaotic regime of the PDNR shown in Fig. 7(a) is generally lower than that in Fig. 7(c). Thus, we observe a larger purity for regular dynamics against chaotic dynamics as we fix the mean oscillatory excitation number within a close range, which indicates a direct relationship between the purity of the state and the underlying oscillatory dynamics.

## IV. SUMMARY

We have demonstrated that the phase-locking phenomenon, which is predicted by the mean-field approximation to arise under the situation of a relatively high photon number in the optical modes, can also occur at the level of a few quanta. In particular, we have explored the formation of phase locking within a nonlinear Kerr oscillator parametrically driven by a train of pulses. We have performed our investigation through the Wigner functions of the cavity mode in phase space for definite time instants with temporal pulses of different widths in both the regular and chaotic regimes. In addition, we have analyzed the photon-number effects of the resonator mode and quantum purity for both operational regimes, which allows us to infer the presence of quantum dissipative chaos. These results have informed us that the phase-locking phenomenon and the quantum statistical effects are cardinally different between the regular and chaotic regimes of the PDNR.

## ACKNOWLEDGMENTS

We acknowledge support from the Armenian State Committee of Science, through Project No. 15T-1C052. G.Y.K. thanks the Nanyang Technological University for hospitality.

[1] Z. R. Lin, K. Inomata, K. Koshino, W. D. Oliver, Y. Nakamura, J. S. Tsai, and T. Yamamoto, Nat. Commun. **5**, 4480 (2014).
[2] R. Islam *et al.*, Opt. Lett. **39**, 3238 (2014).
[3] L. A. Wu, H. J. Kimble, J. L. Hall, and H. Wu, Phys. Rev. Lett. **57**, 2520 (1986).
[4] P. Kinsler and P. D. Drummond, Phys. Rev. A **43**, 6194 (1991).
[5] P. D. Drummond and P. Kinsler, Quantum Semiclass. Opt. **7**, 727 (1995).
[6] P. Kinsler and P. D. Drummond, Phys. Rev. A **52**, 783 (1995).
[7] E. I. Mason and N. C. Wong, Opt. Lett. **23**, 1733 (1998).
[8] C. Fabre, E. I. Mason, and N. C. Wong, Opt. Commun. **170**, 299 (1999).
[9] L. Longchambon *et al.*, Eur. Phys. J. D **30**, 279 (2004).
[10] H. H. Adamyan and G. Yu. Kryuchkyan, Phys. Rev. A **69**, 053814 (2004).
[11] H. H. Adamyan, N. H. Adamyan, S. B. Manvelyan, and G. Yu. Kryuchkyan, Phys. Rev. A **73**, 033810 (2006).
[12] J. Laurat, T. Coudreau, G. Keller, N. Treps, and C. Fabre, Phys. Rev. A **70**, 042315 (2004).
[13] J. Laurat, T. Coudreau, L. Longchambon, and C. Fabre, Opt. Lett. **30**, 1177 (2005).
[14] S. Feng and O. Pfister, Phys. Rev. Lett. **92**, 203601 (2004).
[15] J.-J. Zondy, D. Kolker, and F. N. C. Wong, Phys. Rev. Lett. **93**, 043902 (2004).
[16] G. Yu. Kryuchkyan and N. T. Muradyan, Phys. Lett. **286**, 113 (2001).
[17] G. Yu. Kryuchkyan, L. A. Manukyan, and N. T. Muradyan, Opt. Commun. **190**, 245 (2001).
[18] J. J. Zondy, A. Tallet, E. Ressayre, and M. LeBerre, Phys. Rev. A **63**, 023814 (2001).
[19] D. A. Antonosyan, T. V. Gevorgyan, and G. Yu. Kryuchkyan, Phys. Rev. A **83**, 043807 (2011).
[20] O. Naaman, J. Aumentado, L. Friedland, J. S. Wurtele, and I. Siddiqi, Phys. Rev. Lett. **101**, 117005 (2008).
[21] B. Wielinga and G. J. Milburn, Phys. Rev. A **48**, 2494 (1993).
[22] B. Wielinga and G. J. Milburn, Phys. Rev. A **49**, 5042 (1994).
[23] G. J. Milburn and C. A. Holmes, Phys. Rev. A **44**, 4704 (1991).
[24] G. Yu. Kryuchkyan and K. V. Kheruntsyan, Opt. Commun. **120**, 132 (1996).
[25] K. V. Kheruntsyan, D. S. Krahmer, G. Yu. Kryuchkyan, and K. G. Petrossian, Opt. Commun. **139**, 157 (1997).
[26] C. H. Meaney, H. Nha, T. Duty, and G. J. Milburn, Eur. Phys. J. Quantum Technol. **1**, 7 (2014).
[27] T. V. Gevorgyan and G. Yu. Kryuchkyan, J. Mod. Opt. **60**, 860 (2013).
[28] H. H. Adamyan, S. B. Manvelyan, and G. Yu. Kryuchkyan, Phys. Rev. E **64**, 046219 (2001).
[29] T. V. Gevorgyan, S. B. Manvelyan, A. R. Shahinyan, and G. Yu. Kryuchkyan, in *Modern Optics and Photonics: Atoms and Structured Media*, edited by G. Kryuchkyan, G. Gurzadyan, and A. Papoyan (World Scientific, Singapore, 2010).
[30] T. V. Gevorgyan, A. R. Shahinyan, L. Y. Chew, and G. Yu. Kryuchkyan, Phys. Rev. E **88**, 022910 (2013).
[31] A. Kowalewska-Kudłaszyk, J. K. Kalaga, and W. Leónski, Phys. Rev. E **78**, 066219 (2008).
[32] G. Yu. Kryuchkyan and S. B. Manvelyan, Phys. Rev. Lett. **88**, 094101 (2002).
[33] G. Yu. Kryuchkyan and S. B. Manvelyan, Phys. Rev. A **68**, 013823 (2003).
[34] J. Emerson, Y. S. Weinstein, S. Lloyd, and D. G. Cory, Phys. Rev. Lett. **89**, 284102 (2002).
[35] Y. S. Weinstein, S. Lloyd, and C. Tsallis, Phys. Rev. Lett. **89**, 214101 (2002).

[36] A. Kowalewska-Kudłaszyk, J. K. Kalaga, and W. Leónski, Phys. Lett. A **373**, 1334 (2009).
[37] A. Kowalewska-Kudłaszyk, J. K. Kalaga, W. Leónski, and V. Cao Long, Phys. Lett. A **376**, 1280 (2012).
[38] A. R. Shahinyan, L. Y. Chew, and G. Yu. Kryuchkyan, Phys. Lett. A **377**, 2743 (2013).
[39] S. Kumar and D. P. DiVincenzo, Phys. Rev. B **82**, 014512 (2010).
[40] J. Bourassa, F. Beaudoin, J. M. Gambetta, and A. Blais, Phys. Rev. A **86**, 013814 (2012).
[41] A. Miranowicz, J. Bajer, M. Paprzycka, Y.-X. Liu, A. M. Zagoskin, and F. Nori, Phys. Rev. A **90**, 033831 (2014).
[42] I. C. Percival, *Quantum State Diffusion* (Cambridge University Press, Cambridge, 2000).